

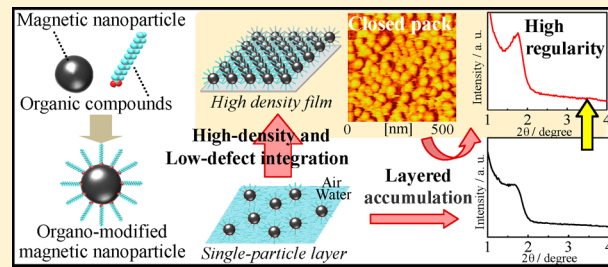
Creation of High-Density and Low-Defect Single-Layer Film of Magnetic Nanoparticles by the Method of Interfacial Molecular Films

Atsuhiro Fujimori,*† Kyohei Ohmura,‡ Nanami Honda,† and Koichi Kakizaki†

†Graduate School of Science and Engineering and ‡Department of Functional Materials Science, Faculty of Engineering, Saitama University, 255 Shimo-okubo, Sakura-ku, Saitama 338-8570, Japan

Supporting Information

ABSTRACT: A technique to solubilize fine magnetic inorganic particles in general organic solvents is proposed via surfaces modification by long-chain carboxylic acids. This organic modification should overcome the relatively weak van der Waals interactions between the nanoparticles, allowing the formation of ordered arrangements of the modified Fe_3O_4 and CoFe_2O_4 materials. Using nanodispersions of these organo-modified magnetic nanoparticles as “spreading solutions”, Langmuir monolayers of these particles were formed. Multiparticle layered structures were constructed by the Langmuir–Blodgett (LB) technique. The fabrication of single- and multiparticle layers of organo-modified magnetic nanoparticles was investigated using surface pressure–area (π –A) isotherms, out-of-plane X-ray diffraction (XRD), in-plane XRD, and atomic force microscopy (AFM). The out-of-plane XRD profile of a single-particle layer of organo-modified Fe_3O_4 clearly showed a sharp peak which was attributed to the distance between Fe_3O_4 layers along the *c*-axis. The AFM image of single-particle layer of organo-modified CoFe_2O_4 revealed integrated particle organization with a uniform height; these aggregated particles formed large two-dimensional crystals. For both nanoparticle species, regular periodic structures along the *c*-axis and high-density single-particle layers were produced via the Langmuir and LB techniques.



INTRODUCTION

Fine particle integration technologies that enable the formation of high-density particle films with few defects constitute an important and basic research area that can contribute to the development of next-generation quantum devices.^{1,2} Recently, integrated nanoparticles (NPs) have received considerable attention because of their potential use in numerous technical applications ranging from organic devices to biomaterials.^{3–6} Homogeneously sized particles of inorganic oxides such as silica, titania, and zirconia are readily available and have been used as filling and polishing agents,^{7,8} photocatalysts,⁹ and high-refractive-index materials, respectively.^{10,11} However, due to the relatively weak interactions between these inorganic fine particles, hybridization with organic compounds has been studied to improve their properties. Recently, the high-density integration of NPs with a hydrophobic polymer has been achieved at an air/water interface.^{12,13} Further, organic/inorganic hybrid materials^{14,15} have attracted significant attention from scientists as well as engineers owing to their remarkably high-dimensional stability and gas-barrier performance, in addition to their better mechanical properties than conventional composite materials.^{16,17} Another functional material of interest to researchers consists of magnetic nanoparticles (MNPs), which have been used in multiple and varied applications: the isolation of specific biomolecules (screening),¹⁸ in drug transport and cell manipulation,¹⁹ as a minimally invasive cancer treatment that is less arduous for the

patient (magnetic hyperthermia),²⁰ and as clinical MRI contrast agents²¹ because of their controllable flocculation and dispersion properties in solution.²² Their potential for movement and transport by a magnetic field gradient,²³ heat generation by an alternating magnetic field,²⁴ and ability to generate a magnetic field in the surrounding environment²⁵ are also of great interest. More recently, the analysis of interactions at the air/water interface between oleic acid-modified triiron tetroxide NPs and phosphonium lipids has been performed in order to elucidate the influence of the MNPs on the organism.²⁶ In addition, if a high-density, low-defect single-particle layer can be formed by the interfacial integration of biocompatible magnetic fine particles and be vertically accumulated (Figure 1), then such constructs could lead to next-generation high-density perpendicular magnetic recording media.^{27,28}

The two-dimensional integration of MNPs should make it possible to enhance several material functionalities. However, it is difficult to obtain regular arrangements of MNPs because the van der Waals interactions of these inorganic materials are relatively weak. To overcome this limitation, surface modification using organic compounds is an efficient way to increase interparticle affinity. In a previous study, the formation

Received: January 20, 2015

Revised: February 28, 2015

Published: March 1, 2015

and structure of molecular films made of organo-modified montmorillonite were investigated.^{29,30} This organo-modified inorganic material formed an extremely condensed monolayer on a water surface. Further, a highly ordered layer structure along the *c*-axis and two-dimensional packing in the *ab*-plane were commonly constructed by the Langmuir–Blodgett (LB) technique.^{31,32}

Previously, particle integration and formation of layered organization of organo-modified ZrO particles have been attained by the LB method.^{12,33} Further, Kang et al. have reported formation of single particle layer of oleic acid-modified magnetic particles at air/water interface and observation of surface morphology of its transferred film.³⁴ On the other hand, Vico et al. have performed the investigation of interaction between organo-modified magnetic particles and other organic molecules in mixed monolayers of oleic acid-modified magnetic nanoparticles and the saturated/unsaturated phospholipids.²⁶ In comparison with these previous reports, the novelties of this study corresponds a creation of high-density and low-defect particle organization of organo-modified magnetic particles and precise analysis of their particle arrangement.

In the present study, ultrathin organo-modified magnetic nanoparticle (oMNP) films were constructed by floating Langmuir monolayers composed of triiron tetraoxide (Fe_3O_4)³⁵ or cobalt ferrite (CoFe_2O_4) on water.³⁴ The proposed technique is based on nanodispersions of insoluble inorganic particles obtained by solubilizing them in a general organic solvent. In recent years, the formation of two-dimensional organized films of organo-modified zirconia has been attained by applying this modification method.³³ This inorganic fine-particle nanodispersion can be used as a “spreading solvent” for the Langmuir monolayers. In other words, the formation of LB multilayers from inorganic NPs is made possible by using the proposed technique. In this study, the LB multilayers of the oMNP films were characterized by out-of-plane and in-plane X-ray diffraction (XRD) and atomic force microscopy (AFM). The proposed technique can be expected to facilitate the

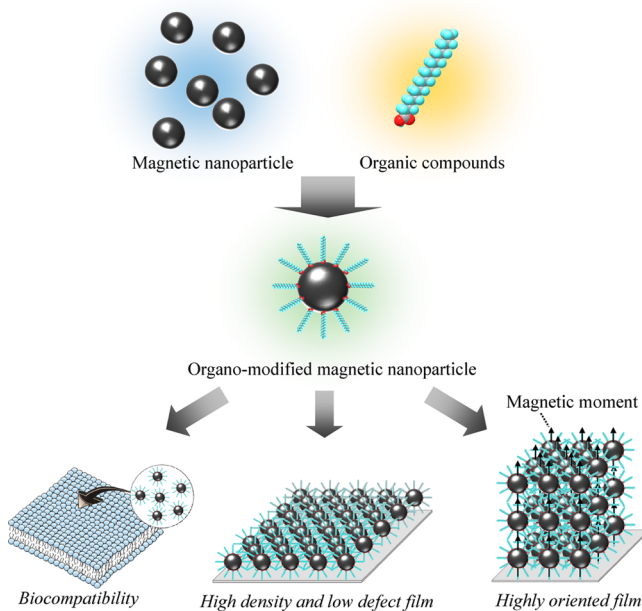


Figure 1. Schematic illustration of formation of organo-modified magnetic nanoparticles.

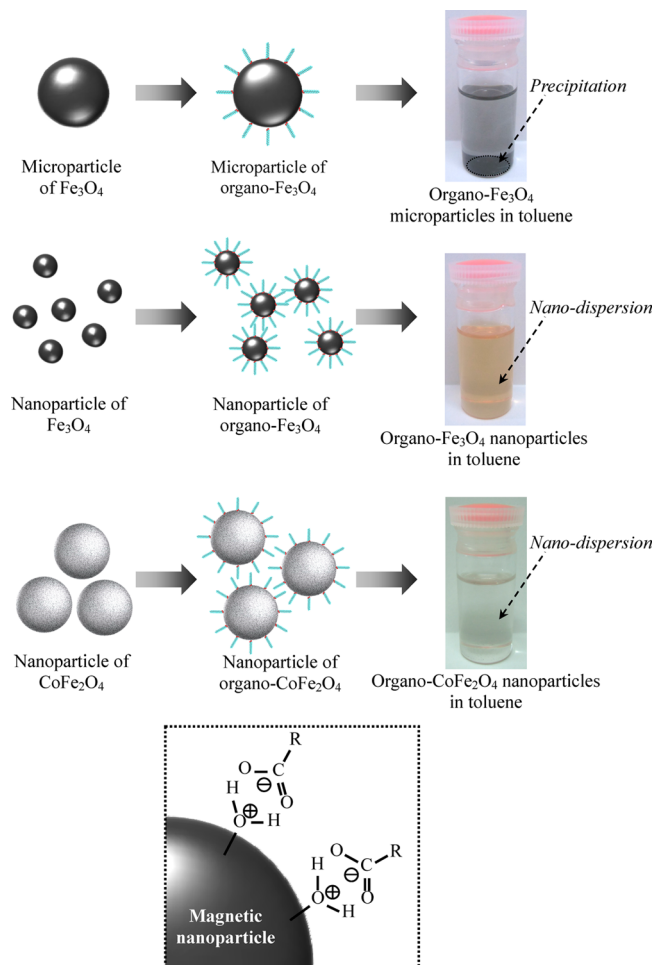


Figure 2. Schematic synthetic process for the organo-modified magnetic particles.

development of a new two-dimensional integration technology for insoluble inorganic NPs using a simple wet process that could be widely employed.

EXPERIMENTAL SECTION

Synthesis and Characterization of Organo-Modified Magnetic Nanoparticles. Figure 2 shows a generalized approach for the preparation of the oMNP, in accordance with the previously reported method.^{12,33} The both MNPs of Fe_3O_4 and CoFe_2O_4 were purchased from Sigma-Aldrich. Organo-modifying agents was stearic acid. A dispersion was prepared by combining an aqueous solution of MNPs (0.5 wt %, 10 mL) with a methanolic solution of stearic acid (8.8×10^{-3} M, 10 mL). Toluene (20 mL) was poured into the MNPs dispersion with stirring. In this step, the oMNP migrated from the methanolic dispersion into the toluene phase. Water, methanol, and the remaining unreacted reagents were then removed by rotary evaporation under reduced pressure and decantation. This process changed the hydroxyl group ($\text{R}-\text{OH}_2^+$) on the particle surface to long-chain alkyl carboxylates. The successful achievement of surface Fe_3O_4 modification depends on the particle size; for example, micron-sized Fe_3O_4 particles aggregate and precipitate from the reaction solution because of their excessively strong interactions. In contrast, 5 nm Fe_3O_4 nanoparticles remain well dispersed in the modification reaction solution, as do 30 nm CoFe_2O_4 NPs.

The oMNP were characterized by IR spectroscopy and powder XRD, which confirmed the successful modification of the 5 nm Fe_3O_4 and 30 nm CoFe_2O_4 particles. The FTIR spectra of oMNP were recorded in the 400–4000 cm^{-1} range (PerkinElmer system, spectrum 2000) by preparing KBr pellets (0.1 wt % sample). In the IR spectra,

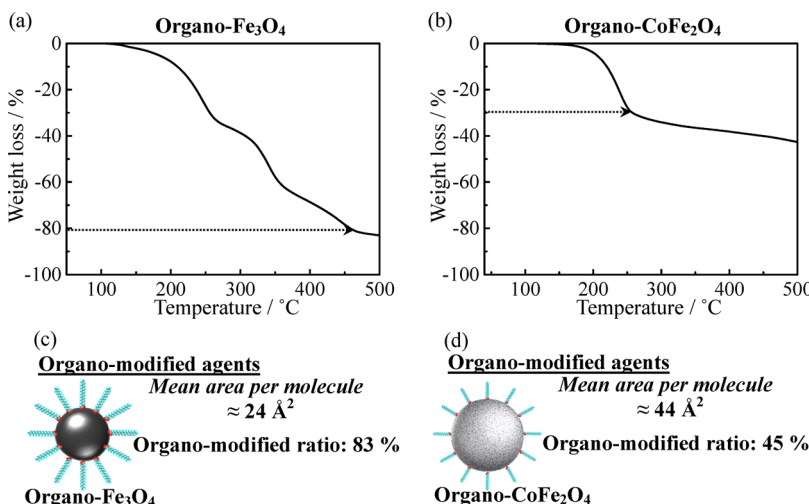


Figure 3. TG curves of (a) organo-modified Fe_3O_4 and (b) organo-modified CoFe_2O_4 . Schematic illustration of (a) organo-modified Fe_3O_4 and (b) organo-modified CoFe_2O_4 with calculated surface coverage.

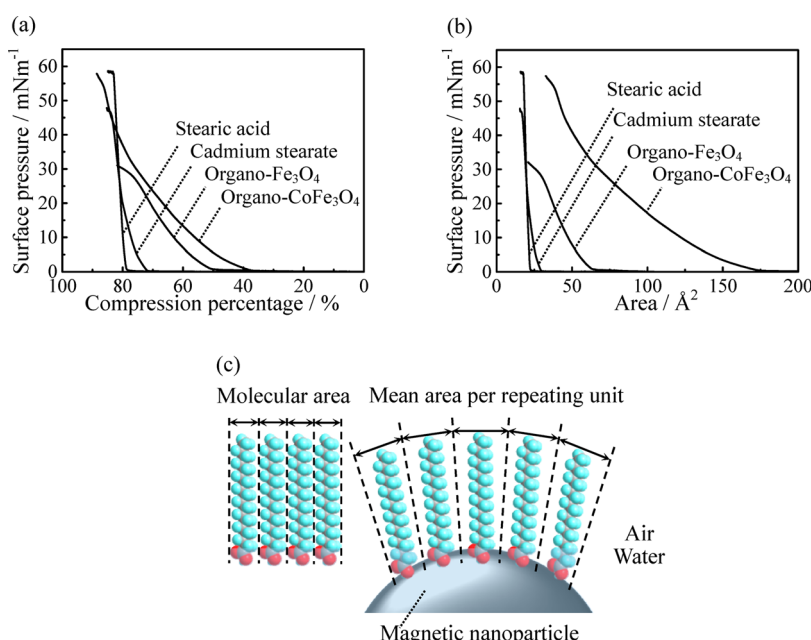


Figure 4. (a) Surface pressure–compression percentage and (b) surface pressure–area (π – A) isotherms of monolayers of cadmium stearate, stearic acid, organo-modified Fe_3O_4 , and organo-modified CoFe_2O_4 on a water surface (15 °C). (c) Schematic illustration of molecular area and mean area per repeating unit in these measurements.

bands derived from the Fe–O lattice vibrations are observed around 580 cm⁻¹ for the Fe_3O_4 and CoFe_2O_4 particles as well as O–H stretching vibrations based on surface-adsorbed water at around 3460 cm⁻¹ (Figure S1a,c in the Supporting Information). In the organo-modified Fe_3O_4 and CoFe_2O_4 NPs, symmetric and asymmetric C–H stretching vibrations derived from the long chain fatty acids are observed near 2840–2910 cm⁻¹.

The samples were characterized for their phase purity and crystallinity by powder X-ray diffraction (XRD) measurements (Rigaku, Rint-Ultima III; Cu K α radiation, 40 kV, 40 mA). The powder XRD profiles revealed that the Fe_3O_4 and CoFe_2O_4 NPs formed cubic spinel crystal structures. In addition, reflections with d spacings of 4.2 Å derived from the long chain fatty acids were confirmed in the organo-modified Fe_3O_4 and CoFe_2O_4 materials (Figure S1b,d in the Supporting Information). Thus, these FTIR and powder XRD results corroborate the incorporation of the organic modifiers.

To estimate the surface coverage, thermogravimetry (TG) was performed on both organo-modified materials (Figure 3). After these samples were dried overnight in a desiccator, TG was done using a Seiko Instruments EXSTART 6200. In Fe_3O_4 and CoFe_2O_4 , the amounts of organic modifier desorbed with increasing temperature were 82 and 29%, respectively. Here, the weights of the particles were calculated using the particle diameters (5 and 30 nm) and densities (5.2 and 5.3 kg/dm³) for Fe_3O_4 and CoFe_2O_4 , respectively. In this case, since adsorbed water layer exists on the surface of the MNPs, a gradual reduction in weight also continues after desorption of the modified alkyl chain. Therefore, a major weight loss approximately considered as desorption of the alkyl chain, and the surface coverages have been calculated by the regarding as desorption temperature at the 450 °C (organo- Fe_3O_4) and 250 °C (organo- CoFe_2O_4), respectively. The existence of the large difference between the desorption temperatures is expected to be due to strong adsorption of carboxyl anions to the surface of Fe_3O_4 MNPs with small diameter. As a result, the surface area coverages by the organic components of the organo-

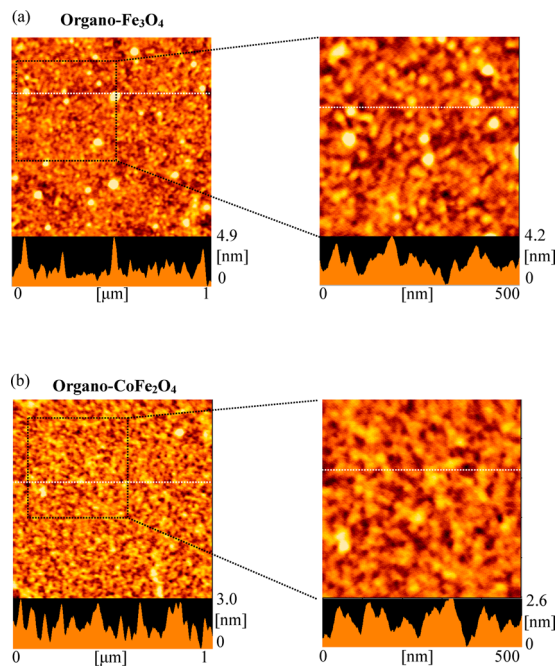


Figure 5. Mesoscopic AFM images of Z-type single-particle layers of (a) organo-modified Fe_3O_4 and (b) organo-modified CoFe_2O_4 transferred by the upstroke LB method.

modified Fe_3O_4 and CoFe_2O_4 are 24 and 44 \AA^2 , respectively. Therefore, the modification ratios are 83 and 45%, respectively.

Formation of Monolayers on Water Surface and Observation of Organo-Nanoparticle Arrangement in Films. Since these oMNPs can be uniformly dispersed in an organic solvent via the proposed process, it is possible to prepare a spreading solvent for the formation of inorganic nanoparticle monolayers on a water surface. Such monolayers were formed by spreading a toluene solution containing the oMNPs (ca. 1.0×10^{-4} M) on distilled water (18.2 $\text{M}\Omega\text{-cm}$). After evaporating toluene for 30 min, surface pressure-area (π -A) isotherms were recorded at a compression speed of 0.08 mm

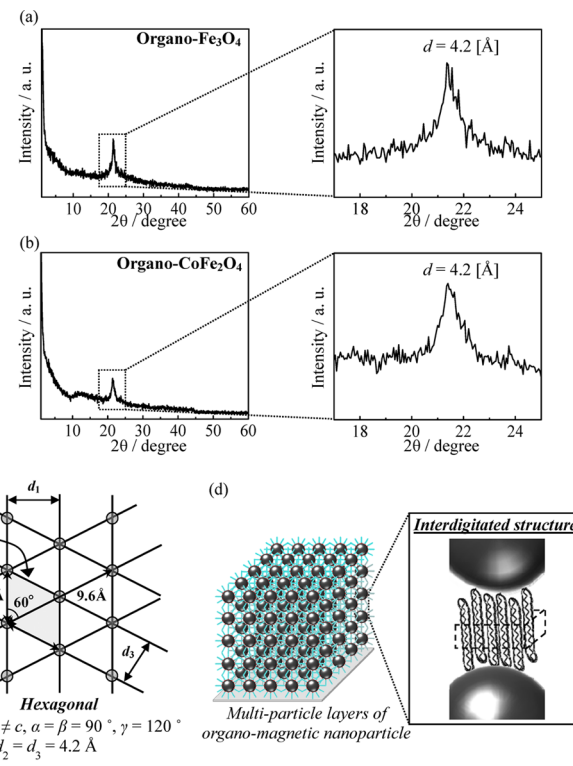


Figure 7. In-plane XRD profiles of multiparticle layers of (a) organo-modified Fe_3O_4 and (b) organo-modified CoFe_2O_4 . (c) Schematic model of two-dimensional lattice formed by long hydrocarbons on the organo-modified magnetic nanoparticle surface of their LB films. (d) Schematic illustration of the formation of the interdigitated structure of the alkyl chain modifiers between particles.

s^{-1} . The temperature of the air/water interface was maintained at a constant value of 15 °C by circulating thermostatically controlled water around the trough. Measurements of the monolayer properties

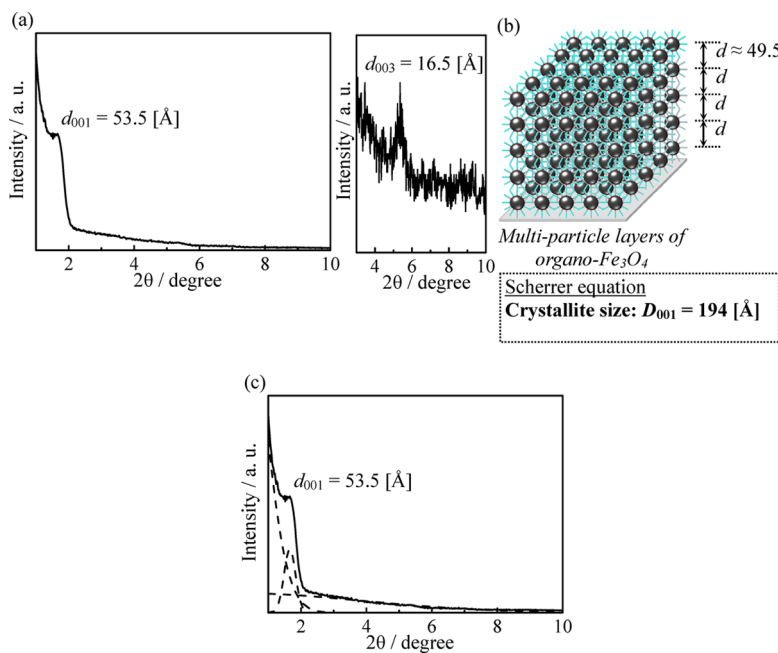


Figure 6. (a) Out-of-plane XRD profiles of multiparticle layers of organo-modified Fe_3O_4 nanoparticles. (b) Schematic illustration of multiparticle layered organization of organo-modified Fe_3O_4 nanoparticles. (c) Deconvolution of d_{001} diffraction peak by Gaussian fitting.

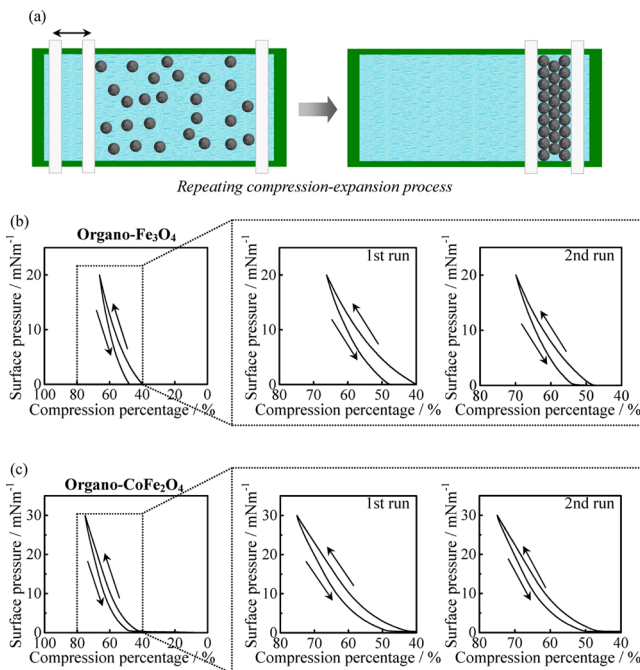


Figure 8. (a) Schematic illustration of the “repeating compression–expansion method.” Hysteresis curves of π –A isotherms of single-particle layers of (b) organo-modified Fe_3O_4 and (c) organo-modified CoFe_2O_4 nanoparticles on a water surface (15°C).

and LB film transfer were carried out using a USI-3-22 Teflon-coated LB trough (USI Instruments).

Surface Morphology and Particle Arrangement in Organized Films. The surface morphologies of the transferred films were observed using a scanning probe microscope (Seiko Instruments, SPA300 with a SPI-3800 probe station) and microfabricated rectangular Si cantilevers with integrated pyramidal tips; a constant force of 1.4 N m^{-1} was applied in this process. The large spacing between the layer structures of the films transferred onto the glass substrates was measured using an out-of-plane X-ray diffractometer (Rigaku, Rint-Ultima III; Cu $\text{K}\alpha$ radiation, 40 kV , 40 mA) equipped with a graphite monochromator. The in-plane spacing of the two-dimensional lattice of the films was determined using a custom-built X-ray diffractometer with different geometrical arrangements^{36,37} (Bruker AXS, MXP-BX; Cu $\text{K}\alpha$ radiation, 40 kV , 40 mA) and equipped with a parabolic graded multilayer mirror. X-rays were incident at an angle of 0.2° , and the films were slow-scanned at a speed of $0.05^\circ/80 \text{ s}$. Thus, in-plane XRD measurements were carried out at monomolecular resolution.

RESULTS AND DISCUSSION

The interfacial monolayer behavior of organo-modified inorganic fine particles is extremely interesting with respect to determining the influence of the monolayer components on its properties. Figures 4a,b show the π –A isotherms of single-particle layers of the MNPs modified by stearic acid on a water surface. The figures also present the monolayer behaviors of the oMNPs, stearic acid, and Cd stearate for comparison. In this case, the concept of molecular weight cannot be applied because the total number of atoms in a magnetic nanoparticle unit cannot be exactly determined. Therefore, considering the surface conformations as shown in Figure 4c, the repeating units of only the stearate group of the organomagnetic nanoparticle surface are shown in Figures 4a,b. However, it is expected that the most accurate comparison would be derived by using the “compression percentage”, which indicates the

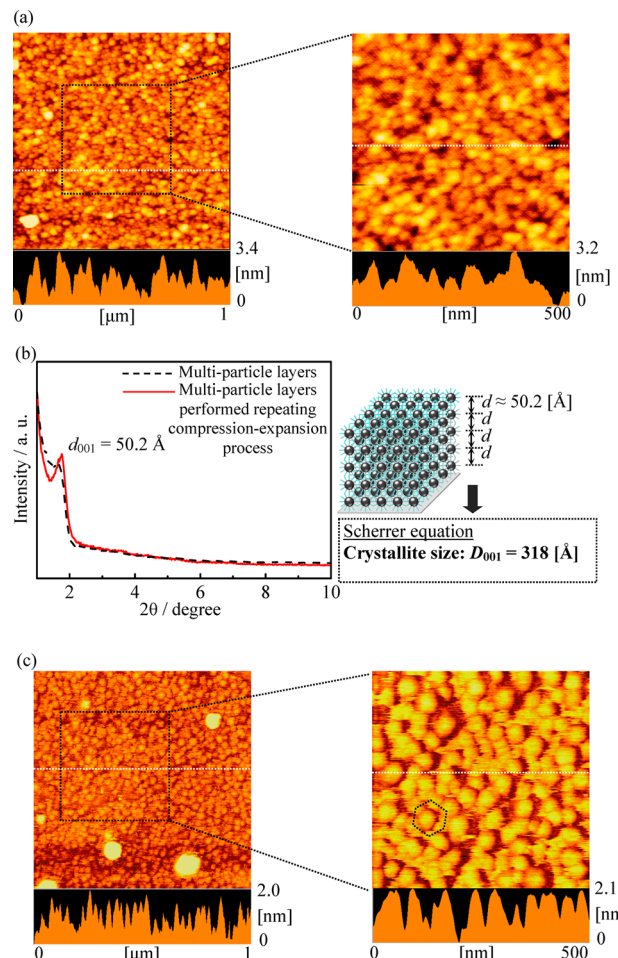


Figure 9. (a) AFM images of a single-particle layer of organo-modified Fe_3O_4 nanoparticles fabricated by “repeating compression–expansion method”. (b) Out-of-plane XRD profiles of multiparticle layers of organo-modified Fe_3O_4 nanoparticle fabricated by “repeating compression–expansion method” with corresponding illustration. (c) AFM images of single-particle layer of organo-modified CoFe_2O_4 fabricated by “repeating compression–expansion method”.

mean of the compression ratio versus the total surface area of the LB trough, as the horizontal axis. Notably, the π –A curves of the oMNPs are clearly different from those of stearic acid and Cd stearate. The horizontal axes in Figures 4a and 4b respectively indicate the “compression percentage” and “area”, where the latter corresponds to an “area per molecule” value in the cases of stearic acid and cadmium stearate and indicates the “mean area per hydrophobic repeating unit” in the case of the MNPs. In addition, only the expanded phases are observed in the π –A curves of monolayers from both oMNPs. Compared to the Fe_3O_4 system, the organo- CoFe_2O_4 monolayer exhibits high values of both the collapse surface pressure and the limiting area.

This single-particle layer on the water surface was transferred to a mica substrate at 15°C by using the upstroke LB method. Single-particle layers of organo-modified Fe_3O_4 and CoFe_2O_4 were transferred at 20 and 30 mN m^{-1} , respectively. Figure 5 shows the AFM images of these Z-type single-particle layers. Unfortunately, it was not possible to obtain a very homogeneous single-particle film at this stage. This problem was eliminated by the “repeating compression–expansion” method (*vide infra*). However, the height of a organo-modified

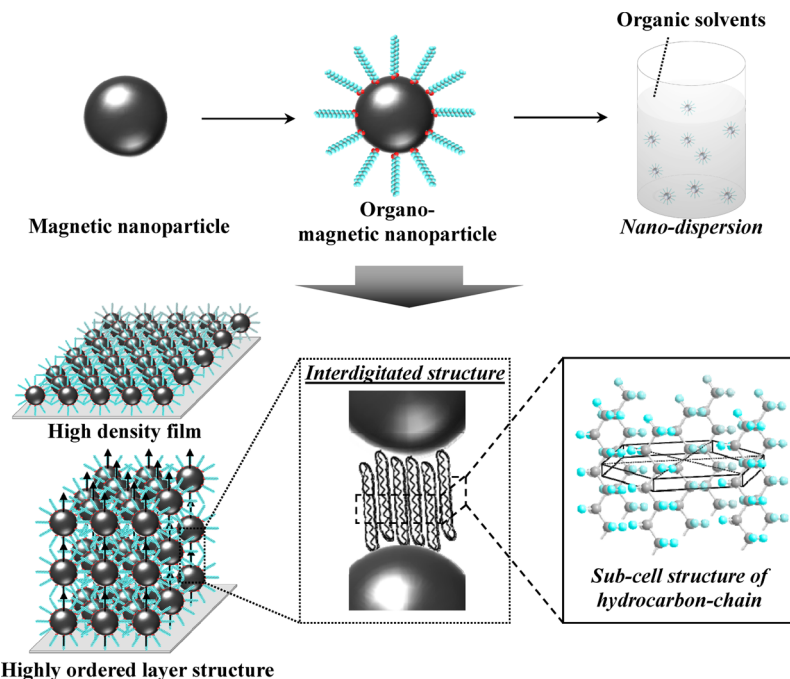


Figure 10. Schematic illustration of the role of the alkyl chain modifier in the formation of organized molecular films of organo-modified magnetic nanoparticles.

Fe_3O_4 single-particle layer was found to be 4–5 nm, which may correspond to the height of a single organo-modified particle. Finally, despite the large particle size, the shape and height information could not be obtained at this stage with respect to the analogous CoFe_2O_4 single-particle layer.

The formation of a quite highly ordered layer arrangement along the vertical direction was inferable from the data in Figure 6a. The results of the out-of-plane X-ray diffraction of the LB multilayers indicate that an organized film of organo-modified Fe_3O_4 was transferred at 15 °C, and the films showed a long-period value at around 5 nm. This value corresponds to the particle lamination period, as shown in Figure 6b. Since the (001) diffraction peak is at a relatively low intensity, it is almost hidden in the direct beam. However, since a third-order reflection is present, it finds that the layered period indicates a high degree of order. In addition, after deconvolution of the (001) diffraction peak from the direct beam and air scattering, Gaussian fitting was performed (Figure 6c). The diameter of the D_{001} microcrystals calculated by the Scherrer equation was nearly 200 Å.

Figure 7 shows the in-plane X-ray diffraction profiles of multiparticle layers of the oMNPs. Unfortunately, the diffraction peak in the low-angle region corresponding to the long spacing in the out-of-plane XRD pattern was not observed. Based on the AFM results, this observation may be reasonable. The arrangement of the particles in the two-dimensional plane would not be highly regular at this stage. However, the long-chain alkyl group modifiers were found to have a high degree of order in the particle layers. A single peak corresponding to the isotropic hexagonal (100) plane was apparent at 4.1 Å in the case of the multiparticle layers fabricated at the subphase temperature of 15 °C. In view of the surface modification ratio of the particles by stearic acid, the possibility that the long alkyl chains are densely packed on one particle surface is extremely low. This inference is obtained by comprehensive analysis of in-plane XRD, out-of-plane XRD, and height information on the

AFM. Accordingly, from the determination by the integrating of these three kinds of analytical results, packing of the alkyl chains is expected to generate a two-dimensional crystal array of the alkyl chains between individual particles. In other words, the two-dimensional integration and formation of the layer structure of oMNPs can be determined, indicating that crystal formation arises from the interactions between the alkyl chain modifiers. This inferred model is represented in Figure 7c. Subcell³⁸ formation by the hydrocarbons between the particles is considered the origin of the integrated nanoparticle organization in this system. Incidentally, the period between the particles of the organo-modified CoFe_2O_4 multiparticle layers exceeds the detection limit of this measurement. However, the details of the long alkyl chain packing are captured analogously to those of the organo-modified Fe_3O_4 multiparticle layers.

As the next step, the formation of high-density, low-defect particle layers was addressed. Figure 8a shows a schematic illustration of a “repeating compression–expansion process” for the generation of a single-particle layer on the water surface. In a system where the size of the components is large and the interaction between constituent units is relatively weak, this process can effectively form low-defect layers. The fact that this technique works effectively reflects the monolayer properties of the inorganic compound. In the case of an organo-modified montmorillonite single-particle layer, this technique was effectively applied in the fabrication of low-defect films.^{29,30} Figures 8b,c illustrate the reversibility and hysteresis of the π -A isotherms at 15 °C. At each step of the repeating process, the difference in the hysteresis during compression–expansion decreases. When this process was performed ten and three times for the organo-modified Fe_3O_4 and CoFe_2O_4 nanoparticles, respectively, the ninth and second curves of the hysteresis loops almost coincided. Therefore, considering that the highest density film of the organo-modified Fe_3O_4 had successfully been attained, the resulting monolayer and LB

multilayers transferred to the solid substrate were subjected to AFM observation and out-of-plane X-ray diffraction. The results confirmed a very-low-defect surface morphology for the organo-modified Fe_3O_4 film (Figure 9a). In addition, the d_{001} peak in the out-of-plane X-ray diffraction pattern of the multiparticle layers became very sharp (Figure 9b), and the calculated D_{001} crystallite size increased over 1.5 times. The AFM image of the high-density monolayer of the organo-modified CoFe_2O_4 , prepared by the “repeating compression–expansion process”, on a solid substrate was obtained (Figure 9c). The formation of a considerably high-density single-particle layer with low defect content can be confirmed, as compared to Figure 5, due to the successful capture of a very clear image of the densely packed, 30 nm particles. A partially pseudohexagonal packing structure was also observed, which remarkably indicates the high regularity of the monolayer.

The findings of this study are summarized in Figure 10. The role of the surface-modifying organic chains was considered based on a two-dimensional integrated layer of the oMNPs and the formation of a highly ordered multiparticle layered assembly. When an amphiphatic long-chain organic compound encounters the inorganic particles at the contact interface, new functionality can be imparted to the inorganic particles. As a result, we were able to create an oriented organization of the oMNPs, which could lead to application as a perpendicular magnetic recording medium.

CONCLUSIONS

In this study, the creation of single- and multiparticle layers of two species of organo-modified magnetic nanoparticles was investigated. The magnetic nanoparticles were solubilized in general organic solvents after surface modification, and single-particle layers could be formed when these nanodispersions were used as “spreading solutions” to form monolayers on the water surface. Modification of the magnetic nanoparticle surface was achieved by using a long-chain carboxylic acid, and ordered arrangements of these modified nanoparticles could be easily attained by overcoming the relatively weak van der Waals interactions between the inorganic particles. Langmuir monolayers of the particles were formed, and a multiparticle layered structure was constructed by the LB technique. The out-of-plane XRD profiles of a single-particle layer of organo-modified Fe_3O_4 clearly showed a sharp peak, attributed to the distance between the Fe_3O_4 layers along the c -axis. The AFM image of single-particle layer of organo-modified CoFe_2O_4 showed an integrated particle organization with a uniform height. These aggregated particles form large two-dimensional crystals. For both modified materials, regular periodic structures along the c -axis and high-density single-particle layers were produced by the Langmuir and LB techniques, respectively.

ASSOCIATED CONTENT

Supporting Information

IR spectra and powder XRD profiles of stearic acid, organo-modified Fe_3O_4 and Fe_3O_4 nanoparticles; IR spectra and powder XRD profiles of stearic acid, organo-modified CoFe_2O_4 , and CoFe_2O_4 nanoparticles. This material is available free of charge via the Internet at <http://pubs.acs.org>.

AUTHOR INFORMATION

Corresponding Author

*Tel and Fax +81-48-858-3503; e-mail fujimori@fms.saitama-u.ac.jp (A.F.).

Notes

The authors declare no competing financial interest.

ACKNOWLEDGMENTS

The authors extend their appreciation to the Ministry of Education, Culture, Sports, Science and Technology (MEXT) for a Grant-in-Aid for Scientific Research (C, 25410219 (A.F.)). In addition, the authors greatly appreciate the information on triiron tetroxide particles supplied by Professor Kenji Kamishima at Saitama University.

REFERENCES

- (1) Hammond, P. T. Form and Function in Multilayer Assembly: New Applications at the Nanoscale. *Adv. Mater.* **2004**, *16*, 1271–1293.
- (2) Khanh, N. N.; Yoon, K. B. Facile Organization of Colloidal Particles into Large, Perfect One- and Two-Dimensional Arrays by Dry Manual Assembly on Patterned Substrates. *J. Am. Chem. Soc.* **2009**, *131*, 14228–14230.
- (3) Xue, M.; Zhang, Z.; Zhu, N.; Wang, F.; Zhao, X. S.; Cao, T. Transfer Printing of Metal Nanoparticles with Controllable Dimensions, Placement, and Reproducible Surface-Enhanced Raman Scattering Effects. *Langmuir* **2009**, *25*, 4347–4351.
- (4) Lvov, Y.; Munge, B.; Giraldo, O.; Ichinose, I.; Suib, S. L.; Rusling, J. F. Films of Manganese Oxide Nanoparticles with Polycations or Myoglobin From Alternate-layer Adsorption. *Langmuir* **2000**, *16*, 8850–8857.
- (5) Zakhidov, A. A.; Baughman, R. H.; Iqbal, Z.; Cui, C.; Khayrullin, I.; Dantas, S. O.; Marti, J.; Ralchenko, V. G. Carbon Structures with Three-dimensional Periodicity at Optical Wavelengths. *Science* **1998**, *282*, 897–901.
- (6) Roberts, G. G. *Langmuir-Blodgett Films*; Plenum Press: London, 1990.
- (7) Petty, M. C. *Langmuir-Blodgett Films*; Cambridge University Press: New York, 1996.
- (8) Liang, C.; Wang, L.; Liu, W.; Song, Z. Non-spherical Colloidal Silica Particles—Preparation, Application and Model. *Colloids Surf., A* **2014**, *457*, 67–72.
- (9) Asahi, R.; Morikawa, T.; Ohwaki, T.; Aoki, K.; Taga, Y. Visible-light Photocatalysis in Nitrogen-doped Titanium Oxides. *Science* **2001**, *293*, 269–271.
- (10) Kim, K. M.; Keum, D. K.; Chujo, Y. Organic-Inorganic Polymer Hybrids Using Polyoxazoline Initiated by Functionalized Silsesquioxane. *Macromolecules* **2003**, *36*, 867–875.
- (11) Naka, K.; Chujo, Y. Control of Crystal Nucleation and Growth of Calcium Carbonate by Synthetic Substrates. *Chem. Mater.* **2001**, *13*, 3245–3259.
- (12) Fujimori, A.; Kaneko, Y.; Kikkawa, T.; Chiba, S.; Shibasaki, Y. Fabrication and Structure of “Polymer Nanosphere Multilayered Organization”. *J. Colloid Interface Sci.* **2014**, *418*, 338–349.
- (13) Fujimori, A.; Sato, N.; Chiba, S.; Abe, Y.; Shibasaki, Y. Surface Morphological Changes in Monolayers of Aromatic Polyamides Containing Various N-Alkyl Side Chains. *J. Phys. Chem. B* **2010**, *114*, 1822–1835.
- (14) Alam, M. M.; Mushfiq, M.; Han, H.; Bhowmik, P. K.; Goswami, K. Design and Synthesis of n-Type Organic-Inorganic Hybrid Material Incorporating CdSe Quantum Dots Nanocrystal Core and Diphenylquinoline Peripheral Group. *Macromolecules* **2008**, *41*, 7790–7793.
- (15) Kagan, C. R.; Mitzi, D. B.; Dimitrakopoulos, C. D. Organic-Inorganic Hybrid Materials as Semiconducting Channels in Thin-Film Field-Effect Transistors. *Science* **1999**, *286*, 945–947.
- (16) Zeng, C.; Lee, L. J. Poly(methyl methacrylate) and Polystyrene/Clay Nanocomposites Prepared by *in-situ* Polymerization. *Macromolecules* **2001**, *34*, 4098–4103.
- (17) Manias, E.; Touney, A.; Wu, L.; Strawhecker, K.; Lu, B.; Chung, T. C. Polypropylene/Montmorillonite Nanocomposites. Review of the Synthetic Routes and Materials Properties. *Chem. Mater.* **2001**, *13*, 3516–3523.

- (18) Katz, E.; Willner, I. Integrated Nanoparticle-Biomolecule Hybrid Systems: Synthesis, Properties, and Applications. *Angew. Chem., Int. Ed.* **2004**, *43*, 6042–6108.
- (19) Kim, J.; Lee, J. E.; Lee, S. H.; Yu, J. H.; Lee, J. H.; Park, T. G.; Hyeon, T. Designed Fabrication of a Multifunctional Polymer Nanomedical Platform for Simultaneous Cancer-Targeted Imaging and Magnetically Guided Drug Delivery. *Adv. Mater.* **2008**, *20*, 478–483.
- (20) Cha, H. G.; Kim, C. W.; Kang, S. W.; Kim, B. K.; Kang, Y. S. Preparation and Characterization of the Magnetic Fluid of Trimethoxyhexadecylsilane-Coated Fe_3O_4 Nanoparticles. *J. Phys. Chem. C* **2010**, *114*, 9802–9807.
- (21) Song, S.; Guo, H.; Jiang, Z.; Jin, Y.; Zhang, Z.; Sun, K.; Dou, H. Self-Assembled Fe_3O_4 /Polymer Hybrid Microbubble with MRI/Ultrasound Dual-Imaging Enhancement. *Langmuir* **2014**, *30*, 10557–10561.
- (22) Zhang, Q.; Thompson, M. S.; Carmichael-Baranauskas, A. Y.; Caba, B. L.; Zalich, M. A.; Lin, Y.-N.; Mefford, O. T.; Davis, R. M.; Riffle, J. S. Aqueous Dispersions of Magnetite Nanoparticles Complexed with Copolyether Dispersants: Experiments and Theory. *Langmuir* **2007**, *23*, 6927–6936.
- (23) Latham, A. H.; Williams, M. E. Controlling Transport and Chemical Functionality of Magnetic Nanoparticles. *Acc. Chem. Res.* **2008**, *41*, 411–420.
- (24) Brulé, S.; Levy, M.; Wilhelm, C.; Letourneur, D.; Gazeau, F.; Ménager, C.; Visage, C. L. Doxorubicin Release Triggered by Alginate Embedded Magnetic Nanoheaters: A Combined Therapy. *Adv. Mater.* **2011**, *23*, 787–790.
- (25) Ullal, A. V.; Reiner, T.; Yang, K. S.; Gorbatov, R.; Min, C.; Issadore, D.; Lee, H.; Weissleder, R. Nanoparticle-Mediated Measurement of Target-Drug Binding in Cancer Cells. *ACS Nano* **2011**, *5*, 9216–9224.
- (26) Matshaya, T. J.; Lanterna, A. E.; Granados, A. M.; Krause, R. W. M.; Maggio, B.; Vico, R. V. Distinctive Interactions of Oleic Acid Covered Magnetic Nanoparticles with Saturated and Unsaturated Phospholipids in Langmuir Monolayers. *Langmuir* **2014**, *30*, 5888–5896.
- (27) Huang, X.; Li, L.; Luo, X.; Zhu, X.; Li, G. Orientation-Controlled Synthesis and Ferromagnetism of Single Crystalline Co Nanowire Arrays. *J. Phys. Chem. C* **2008**, *112*, 1468–1472.
- (28) Chen, D.-H.; Chen, Y.-Y. Synthesis of Strontium Ferrite Ultrafine Particles Using Microemulsion Processing. *J. Colloid Interface Sci.* **2001**, *236*, 41–46.
- (29) Fujimori, A.; Arai, S.; Soutome, Y.; Hashimoto, M. Improvement of Thermal Stability of Enzyme via Immobilization on Langmuir-Blodgett Films of Organo-Modified Aluminosilicate with High Coverage. *Colloids Surf., A* **2014**, *448*, 45–52.
- (30) Fujimori, A.; Arai, S.; Kusaka, J.; Kubota, M.; Kurosaka, K. Formation and Structure of Langmuir-Blodgett Films of Organo-Modified Aluminosilicate with High Surface Coverage. *J. Colloid Interface Sci.* **2013**, *392*, 256–265.
- (31) Blodgett, K. Monomolecular Films of Fatty Acids on Glass. *J. Am. Chem. Soc.* **1934**, *56*, 495–495.
- (32) Ulman, A. *An Introduction to Ultrathin Organic Films: from Langmuir-Blodgett to Self-assembly*; Academic Press: Boston, 1991.
- (33) Fujimori, A.; Honda, N.; Iwashia, H.; Kaneko, Y.; Arai, S.; Sumita, M.; Akasaka, S. Formation and Structure of Fine Multi-particle Layered Organo-Modified Zirconium Dioxides Fabricated by Langmuir-Blodgett Technique. *Colloids Surf., A* **2014**, *446*, 109–117.
- (34) Lee, D. K.; Kim, Y. H.; Kang, Y. S.; Stroeve, P. Preparation of a Vast CoFe_2O_4 Magnetic Monolayer by Langmuir-Blodgett Technique. *J. Phys. Chem. B* **2005**, *109*, 14939–14944.
- (35) Lee, D. K.; Kim, Y. H.; Kim, C. W.; Cha, H. G.; Kang, Y. S. Vast Magnetic Monolayer Film with Surfactant-Stabilized Fe_3O_4 Nanoparticles Using Langmuir-Blodgett Technique. *J. Phys. Chem. B* **2007**, *111*, 9288–9293.
- (36) Fujimori, A.; Sugita, Y.; Nakahara, H.; Ito, E.; Hara, M.; Matsui, N.; Kanai, K.; Ouchi, Y.; Seki, K. Change of Molecular Packing and Orientation From Monolayer to Multilayers of Hydrogenated and Fluorinated Carboxylates Studied by In-plane X-ray Diffraction together with NEXAFS Spectroscopy at C K-Edge. *Chem. Phys. Lett.* **2004**, *387*, 345–351.
- (37) Fujimori, A.; Araki, T.; Nakahara, H.; Ito, E.; Hara, M.; Ishii, H.; Ouchi, Y.; Seki, K. In-Plane X-ray Diffraction and Polarized NEXAFS Spectroscopic Studies on the Organized Molecular Films of Fluorinated Amphiphiles with Vinyl Esters and Their Comb-Polymers. *Chem. Phys. Lett.* **2001**, *349*, 6–12.
- (38) Vand, V.; Bell, I. P. A Direct Determination of the Crystal Structure of the β Form of Trilaurin. *Acta Crystallogr.* **1951**, *4*, 465–469.